CATHODE SPUTTERING OF SINGLE-CRYSTAL BALLS

V. E. YURASOVA and I. G. SIROTENKO

Moscow State University

Submitted to JETP editor April 27, 1961

J. Exptl. Theoret. Phys. (U.S.S.R.) 41, 1359-1364 (November, 1961)

Single-crystal balls of copper, tungsten, chromium, iron, cobalt, and germanium and of indium-antimony alloy were bombarded with 1—10 kev krypton ions. The sputtered material was deposited on a spherical or a cylindrical surface, and the emission directions of sputtered particles were determined. Substances with diamond-type and face-centered cubic lattices were sputtered predominantly in the [110] and [100] directions, whereas for metals with body-centered cubic lattices the [111] and [100] directions were predominant. The deposited patches were more clearly defined than when plane single crystals are sputtered. Photometric measurements indicated that the density decreased from the center to the edge of a patch more rapidly than by a cosine law. The dependence of cathode sputtering anisotropy on crystal structure, atomic number, temperature, and sputtering coefficient is discussed.

INTRODUCTION

WHEN metal single crystals are bombarded with ions, sputtered material is concentrated on the collector in separate well-defined spots.[1] At ion energy close to threshold the spots are formed by atoms ejected only in close-packed crystallographic directions. With increasing ion energy the target material also begins to be sputtered in other directions.[2] For example, when the (111) plane of a face-centered lattice is sputtered the deposition pattern consists of six spots instead of the three spots observed at low energies. The three new spots are assigned by different authors to different directions: by Henschke[3] to the [112] direction, by Koedam and Hoogendoorn[4] to [114], and by the authors of [2] to [100].

The disagreement between the interpretations evidently results from the fact that the angles between the directions corresponding to different spots were not determined very accurately. The arrangement and shapes of the patches are affected by the position of the sample with respect to the collector, by the angle that the dominant sputtering direction makes with the ion beam (α_1) and with the sputtered plane (α_2), and also by effects arising when a small area to be sputtered is delimited by Aquadag or a mica diaphragm.

Some of the foregoing difficulties disappear when spherical single crystals are used and the sputtered material is deposited on a spherical collector. In this case all directions (whether close-packed or not) of particle ejection are equivalent with respect to the ion beam direction and the orientation of the target surface. The use of a spherical sample makes it unnecessary to limit the target area with a diaphragm. Also, it becomes possible to detect and index easily a considerably larger number of spots corresponding to definite crystallographic directions than for a plane target.

EXPERIMENTAL PROCEDURE

The cathode sputtering of single-crystal balls of copper, tungsten, chromium, iron, cobalt, and germanium and of an indium-antimony alloy was performed in a low-pressure plasma of high density (at a krypton pressure of $\sim 5 \times 10^{-3}$ mm Hg), with a current of 1—2 amp between the anode and cathode. Spherical samples with 3—6 mm diameters were mounted in the tube through a ground-glass joint and were surrounded by a spherical glass bulb with diameter from 18 to 35 mm. Samples introduced into the plasma in the manner of a Langmuir probe were maintained at a high negative voltage of from 1 to 10 kv. The current density to the sample was usually 5—7 ma/cm^2, and in some experiments reached 13—15 ma/cm^2. The sputtering time varied from a few minutes to two hours. Krypton ions always struck the target perpendicularly, since the thickness of the Langmuir sheath around the sample was less than the mean free path of bombarding ions.

Deposited spots were indexed according to their relative arrangement (pattern symmetry) and angles. For a known radius of the glass bulb the angles were determined from the separation of spots on the spherical surface of the bulb. Since spots on the spherical bulb could not be scanned photometrically, in some instances the glass spheres were replaced with mica cylinders, on which undistorted spots were deposited around the equator of the single-crystal ball. The mica was then unrolled and the spots were scanned photometrically.

Cathode sputtering as a function of temperature was studied as the balls were heated by the ion bombardment. The temperature of a ball was measured by comparing its glow with that of an adjacent tungsten filament 0.1 mm thick. The filament temperature was known from a calibration table as a function of current.

RESULTS

1. Sputtering of face-centered cubic single-crystal balls of Cu and β-Co. After a copper ball of 4-mm diameter had been sputtered for 15 minutes the glass collector of 35-mm diameter revealed well-defined equally spaced spots (Fig. 1a). The angles between all nearest directions of deposition were 60°, i.e., all spots represented sputtering in the [110] direction. When the sputtering period is a few times longer an additional series of spots is observed; these are considerably less defined and broader than those in the [110] direction. The directions of the new spots are 45° from the [110] direction; they therefore represent sputtering in the [100] direction (Fig. 1b). The spots in the [112] or [114] directions that are mentioned in [3] and [4] were not observed in the sputtering of a copper ball.

A similar pattern consisting of spots in the [110] direction was obtained by sputtering a face-centered β-Co single crystal, although the individual spots were considerably less well defined than in the case of Cu.

In the experiments with a copper ball it was noticed that patch size decreases as the collector approaches the ball, and that the patches can even become smaller than the diameter of the ball. Figure 2 shows spots on an unrolled cylindrical collector which had been positioned eccentrically with respect to the ball. The smallest spots, which were obtained at a distance of 6 mm from the Cu ball, had one-half the diameter of the latter. Somewhat larger spots were produced at 11 mm separation.

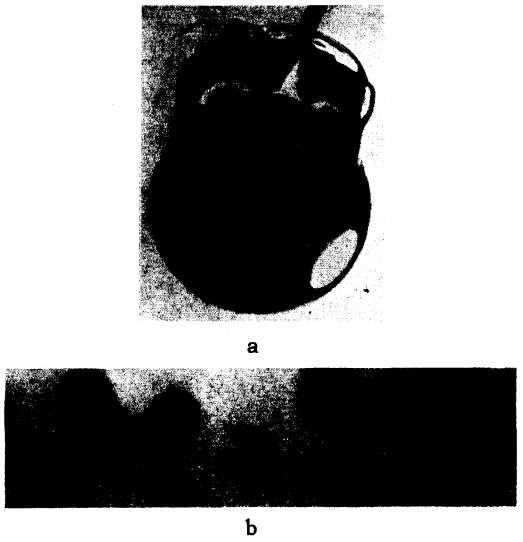

a

b

FIG. 1. a – spots formed on a spherical collector by sputtering a single-crystal copper ball; b – spots of sputtered copper on an unrolled cylindrical collector. Spot 1 corresponds to the [100] direction; the other spots correspond to [110].

The production of spots with diameters smaller than that of the target sphere evidently resulted from the fact that at incident ion energies greater than 1 kev perpendicular ejection from the surface is favored, all other conditions being equal, over oblique ejection. Therefore sputtering in a given crystallographic direction originates most efficiently on a small region of the spherical surface from which particles are ejected close to the normal.

Photometric scanning showed that on spots in the [110] direction, which were very much more clearly defined than when a plane was sputtered, the deposit density decreases from the center to the periphery considerably more rapidly than by a cosine law. The density distribution in the [100] direction is close to a cosine law.

2. Sputtering of body-centered cubic single-crystal balls of Fe, Cr, and W. Ion bombardment of Fe, Cr, and W balls resulted in identical patterns on a spherical collector. Each pattern consisted of two series of spots: a) small but very well defined spots separated by angles of 70° (the [111] direction), and b) larger and somewhat dif-

FIG. 2. Deposition pattern on an unrolled cylindrical collector that had been positioned eccentrically with respect to the copper ball.

FIG. 3. Spots formed on a cylindrical collector by sputtering a single-crystal tungsten ball. Spot 1 corresponds to the [111] direction; spot 2 corresponds to [100].

fuse spots separated by 90° (the [100] direction). This difference between spots in the [111] and [100] directions appears in Fig. 3 and in the photometric curves 1 and 2 of Fig. 4. The most clearly defined pattern was obtained for W, and the least well defined for Fe.

Tungsten was sputtered at different temperatures. At 1300° C the spots were more sharply defined than when the target was heated to only 200 —300° by ion bombardment (curves 2 and 3 in Fig. 4). At higher temperatures two processes occur. First, various impurities are removed from the surface, thus enhancing the sharpness of the pattern; secondly, atomic oscillations around their equilibrium positions are intensified, thus impairing the sharpness of the pattern. At ~ 1300° the first process probably prevails in W.

3. Sputtering of single-crystal balls of Ge and InSb (diamond-type lattice). Wehner[1] has shown that when plane faces of a Ge single crystal are sputtered particles are ejected predominantly in the [111] direction. When we sputtered Ge balls, using a spherical collector, we observed spots in the [110] and [100] directions.

The same result was obtained when an indium-antimony alloy was sputtered (Fig. 5a), although spots in the [110] and [100] directions were more sharply defined than in the case of Ge sputtering.

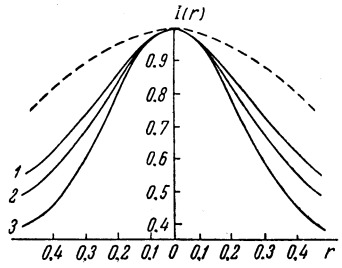

FIG. 4. Photometric density curves of separate spots produced by sputtering a single-crystal tungsten ball. Dashed curve — cosine law. Experimental curves for spots at 200°: 1 — in the [100] direction; 2 — in the [111] direction. At 1300°: 3 — in the [111] direction. The ordinate I(r) is proportional to the density at points of the collector, in relative units.[2] The abscissa is r = x/d, where x is the distance from the center of the spot to the given point in the scanning direction, and d is the distance between the target and collector. The same notation is used in Fig. 5b.

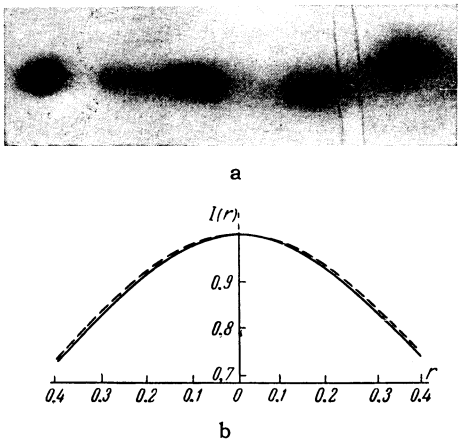

FIG. 5. a — spots in the [110] direction on a cylindrical collector, obtained by sputtering InSb; b — result obtained by photometric scanning of Fig. 5 a. The dashed curve represents a cosine law.

The pattern obtained from a diamond-type lattice is considerably less well defined than from body-centered and face-centered lattices. This could result from the fact that the lattice constant, and therefore the separation of neighboring atoms, in the predominant sputtering directions from the diamond-type lattices of Ge and InSb is considerably larger than in the case of the other metals. The density distribution of the deposit in the [110] direction for InSb is well fitted by a cosine law (Fig. 5b).

DISCUSSION OF RESULTS

The predominant crystallographic directions of single-crystal sputtering and a number of other characteristics are best accounted for by the focusing effect[5,6] arising in some instances of collisions between heavy particles (atoms or ions) in solid matter.

When a solid is irradiated with a stream of heavy particles (specifically, in ion bombardment) atoms of the target are displaced. The moving particles bring about displacements mainly through elastic collisions. Over a broad energy range of incident particles (up to several times ten kev for heavy atoms) the interaction between the incident particles and target atoms (and also the interaction between displaced and fixed atoms) can be calculated quite accurately using the model of elastic solid spheres.

The effective diameter r_0 of a solid sphere depends on the incident-particle energy E, and is determined from the expression for the potential V(r) describing the field due to the charges of the nuclei and electron shells of the interacting atoms. In the first approximation r_0 is deter-

mined from $V(r_0) = E/2$.[5] It is difficult to obtain an exact expression for $V(r)$. Bohr's analysis[7] gives

$$V(r) = \frac{z_1 z_2 \cdot e^2}{r} e^{-r/a}, \quad (1)$$

where z_1 and z_2 are the charges of the moving and fixed nuclei, a is the screening constant, and r is the distance between the centers of the moving and the fixed particle. For the special case of copper bombardment Huntington[8] found that a good approximation of the potential is given by

$$V(r) = 0.038 \exp[-17.2(r-d)/d]\,\text{ev}, \quad (2)$$

where d is the distance to the nearest neighboring atom which is in its equilibrium position.*

The equation $V(r_0) = E/2$ thus determines the effective diameter of a solid atomic sphere of copper for different ion energies. The results for some small values of E are given in the table, where d is taken to be the smallest distance between copper atoms in the [110] direction (2.55×10^{-8} cm).

Silsbee's analysis[5] shows that in some instances where r_0 is close to d and where d is small (i.e., where d/r_0 exceeds unity by an insignificant amount), the moving particle transfers its momentum to the fixed atom in such a way that displacement occurs mainly along close-packed rows of the crystal lattice (the focusing effect). Silsbee's focusing condition is

$$1 < d/2 < 2 \quad (3)$$

and is satisfied for copper atoms in the [110] direction when E is small. When (3) is fulfilled in the [110] direction for copper atoms, focusing in the [100] direction is impossible, according to Silsbee's theory, because a particle displaced in the latter direction must collide with an atom in a [110] row before it reaches an atom in the [100] row.

A more rigorous analysis, however, can also account for the experimentally observed focusing in the [100] direction. It has recently been shown[9,10] that when interactions between neighboring atoms are taken into account focusing is also possible (although less efficient) in directions other than those of close packing.

For body-centered crystals (3) can also be fulfilled in the [100] direction, although not so well as in the close-packed [111] direction. Sputtering in the second most closely packed direction [100] is therefore probably more efficient for body-centered crystals than for face-centered crystals,

*A potential similar to (2) can also be obtained for copper from (1), subject to the condition that r is close to d/2.[6]

E, ev	r_0, Å	d/r_0
11.6	2.23	1.41
50	1.57	1.80
100	1.51	1.69
400	1.28	1.99

as we have observed experimentally. The emission in the [110] and [100] directions from the diamond-type lattices of Ge and InSb is not accounted for by the focusing effect. Equation (3) is not fulfilled for either of these directions; otherwise the spheres of two neighboring atoms separated by the distance $a\sqrt{3/4}$ in the [111] direction would overlap. In this case, to account for focusing in the [110] and [100] directions we must use the more rigorous analysis of Vineyard et al.[10]

As already mentioned, the focusing effect is possible only at low energies of the moving particles. However, preferentially directed ejection from sputtered single crystals is also observed at high incident-ion energies of the order of several times ten kev.[2] Yet even at high primary energies most displacements of atoms from crystal sites are produced by slow particles, very many more of which are present in matter than fast particles.

Therefore even in the case of sputtering by fast ions directed ejection can result from the focusing effect.

Equation (1) shows that the effective radius r_0 of a solid sphere depends in general not only on E but also on the nuclear charges z_1 and z_2 of both the moving and fixed particles, respectively. r_0 increases with z_1 and z_2, so that the focusing condition should be satisfied best by substances with large values of z_2. This agrees with the experimental results for W and Cr sputtering. These two metals have approximately identical values of the sputtering coefficient N, but the lattice constant of W is larger than that of Cr. Nevertheless, the spot pattern for W is more clearly defined than for Cr. This can possibly be associated with the fact that the radius r_0 for W, all other conditions being equal, is considerably larger than for Cr (since $z_W > z_{Cr}$). A similar explanation is perhaps possible for the fact that InSb produces a clearer pattern than Ge, although in this case the results are also affected by the circumstance that N is larger for InSb than for Ge.

It appears from the experimental results that some relation exists between the magnitude of

the sputtering coefficient and the distinctness of spots for different substances. For example, Cr and Fe have identical lattice structures and very close values of both the lattice constant a and nuclear charge z_2. Yet $N_{Cr} > N_{Fe}$, and this can possibly account for the fact that the spot pattern is more clearly defined for Cr than for Fe. The same conclusion can be reached by comparing the sputtering patterns for face-centered cubic crystals (Cu and β-Co), which have close values of a and z_2. In this case $N_{Cu} > N_{Co}$ and therefore the spots are more clearly defined for Cu than for β-Co. For large values of N and at high ion current densities the surface layers of the target are removed more rapidly. This can possibly result in clearer sputtering patterns.

CONCLUSIONS

When face-centered metal lattices are sputtered by krypton ions having energies up to 10 kev, particles are ejected mainly in the close-packed [110] direction, and only to a very small extent in the [100] direction. For metals with body-centered lattices the [111] and [100] directions are predominant, and for diamond-type crystals the predominant directions are [110] and [100].

The patterns of sputtered deposits are most clearly defined for face-centered lattices and are least clear for diamond-type crystals. For the latter the density distribution in individual spots nearly obeys a cosine law, whereas for the former lattices the density decreases much more rapidly with increasing distance from the center of a spot.

When sputtered patterns are compared, a greater relative sharpness is found to accompany a larger sputtering coefficient, a larger atomic number, or a smaller lattice constant of the target (other conditions being identical). The definition is also improved by a temperature rise, within certain limits.

Many results can be accounted for by a focusing effect (according to Silsbee), which should occur under certain conditions if the interaction between moving and stationary atoms is regarded as a two-body collision of elastic solid spheres.

In conclusion the authors wish to thank Professor G. V. Spivak for a valuable discussion, and V. M. Bukhanov for experimental assistance.

[1] G. K. Wehner, Phys. Rev. **102**, 690 (1956).
[2] Yurasova, Pleshivtsev, and Orfanov, JETP **37**, 966 (1959), Soviet Phys. JETP **10**, 689 (1960).
[3] E. B. Henschke, J. Appl. Phys. **28**, 411 (1957).
[4] M. Koedam and A. Hoogendoorn, Physica **26**, 351 (1960).
[5] R. H. Silsbee, J. Appl. Phys. **28**, 1246 (1957).
[6] G. Leibfried, J. Appl. Phys. **30**, 1388 (1959).
[7] N. Bohr, Kgl. Danske Videnskab. Selskab, Mat.-fys. Medd. **18**, No. 8 (1948).
[8] H. B. Huntington, Phys. Rev. **91**, 1092 (1953).
[9] Gibson, Goland, Milgram, and Vineyard, Phys. Rev. **120**, 1229 (1960).
[10] Vineyard, Gibson, Goland, and Milgram, Bull. Am. Phys. Soc. **5**, 26 (1960).

Translated by I. Emin
234

ERRATA

Vol	No	Author	page	col	line	Reads	Should read
13	2	Gofman and Nemets	333	r	Figure	Ordinates of angular distributions for Si, Al, and C should be doubled.	
13	2	Wang et al.	473	r	2nd Eq.	$\sigma_\mu = \frac{e^2f^2}{4\pi^3}\omega^2(\ln\frac{2\omega}{m_\mu} - 0.798)$	$\sigma_\mu = \frac{e^2f^2}{9\pi^3}\omega^2\left(\ln\frac{2\omega}{m_\mu} - \frac{55}{48}\right)$
			473	r	3rd Eq.	$(e^2f^2/4\pi^3)\,\omega^2 \geqslant \ldots$	$(e^2f^2/9\pi^3)\,\omega^2 \geqslant \ldots$
			473	r	17	242 Bev	292 Bev
14	1	Ivanter	178	r	9	1/73	1.58×10^{-6}
14	1	Laperashvili and Matinyan	196	r	4	statistical	static
14	2	Ustinova	418	r	Eq. (10) 4th line	$[-\frac{1}{4}(3\cos^2\theta - 1)\ldots$	$-[\frac{1}{4}(3\cos^2\theta - 1)\ldots$
14	3	Charakhchyan et al.	533		Table II, col. 6 line 1	1.9	0.9
14	3	Malakhov	550		The statement in the first two phrases following Eq. (5) are in error. Equation (5) is meaningful only when s is not too large compared with the threshold for inelastic processes. The last phrase of the abstract is therefore also in error.		
14	3	Kozhushner and Shabalin	677 ff		The right half of Eq. (7) should be multiplied by 2. Consequently, the expressions for the cross sections of processes (1) and (2) should be doubled.		
14	4	Nezlin	725	r	Fig. 6 is upside down, and the description "upward" in its caption should be "downward."		
14	4	Geĭlikman and Kresin	817	r	Eq. (1.5)	$\ldots\left[b^2\sum_{s=1}^{\infty}K_2(bs)\right]^2$	$\ldots\left[b^2\sum_{s=1}^{\infty}(-1)^{s+1}K_2(bs)\right]^2$
			817	r	Eq. (1.6)	$\Phi(T) = \ldots$	$\Phi(T) \approx \ldots$
			818	l	Fig. 6, ordinate axis	$\frac{\varkappa_s(T)}{\varkappa_n(T_c)}$	$\frac{\varkappa_s(T)}{\varkappa_n(T)}$
14	4	Ritus	918	r	4 from bottom	two or three	2.3
14	5	Yurasov and Sirotenko	971	l	Eq. (3)	$1 < d/2 < 2$	$1 < d/r < 2$
14	5	Shapiro	1154	l	Table	2306	23.6